SYNTHESIS AND ELECTROCHEMICAL REDUCTION OF METHYL 3-HALO-1-BENZOTHIOPHENE-2-CARBOXYLATES

Michal Rejňák[a,b], Jiří Klíma[b1], Jiří Svoboda[a1] and Jiří Ludvík[b2,*]

[a] *Department of Organic Chemistry, Institute of Chemical Technology, Prague, Technická 5, 166 28 Prague 6, Czech Republic; e-mail:* [1] *jiri.svoboda@vscht.cz*

[b] *J. Heyrovský Institute of Physical Chemistry and Electrochemistry, Academy of Sciences of the Czech Republic, Dolejškova 3, 182 23 Prague 8, Czech Republic; e-mail:* [1] *jiri.klima@jh-inst.cas.cz,* [2] *jiri.ludvik@jh-inst.cas.cz*

Received July 11, 2003
Accepted October 23, 2003

Dedicated to Professor Rudolf Zahradník on the occasion of his 75th birthday.

A preparative method of synthesis of the new methyl 3-iodo-1-benzothiophene-2-carboxylate was elaborated. Electrochemical behavior of methyl 3-chloro-, bromo- and iodo-1-benzothiophene-2-carboxylates **1**–**3**, and of their reduction and dimer products **4**, **5** in anhydrous dimethylformamide has been investigated at mercury and platinum electrodes using polarography, cyclic voltammetry and voltammetry on a rotating platinum disk electrode. The reduction in divided cells follows the ECE mechanism (electron – chemical step – electron), where the primary radical anion is split into a halide anion and neutral heterocyclic radical, which is immediately reduced by the second electron and protonated. The only reduction product is the methyl 1-benzothiophene-2-carboxylate (**5**); whereas the EDim mechanism (electron – dimer formation) leading to the dimeric species **4** was not observed under the above conditions. Reduction of **1**–**3** on platinum causes formation of a blocking film on the electrode. Sonication during electrolysis successfully reactivates the electrode.

Keywords: Halobenzothiophenes; Biaryls; Voltammetry; Electroreduction mechanism; Mercury and platinum electrodes; Adsorption; Sonication; Electrochemistry.

Formation of an aryl–aryl bond can be accomplished by various methods, especially by transition metal-catalyzed coupling reactions of haloarenes[1–4]. Synthesis of biaryls is of a great interest because they found broad application[5–7] as chiral templates for stoichiometric and asymmetric catalytic reactions and also in designing new materials with liquid-crystalline properties[8–10]. Recently[11] we successfully used the classic Ullman reaction of easily accessible methyl 3-chloro-[12,13] (**1**) and 3-bromo-1-benzothiophene-2-carboxylates[14–16] (**2**) (Scheme 1) for an efficient preparation of 3,3′-bi(1-benzo-

thiophene) derivative **4** and designed a new chiral reducing agent possessing an axially chiral 3,3′-bi(1-benzothiophene) ligand.

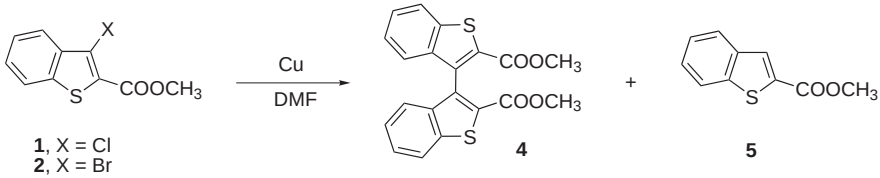

1, X = Cl
2, X = Br
3, X = I

4 **5**

SCHEME 1

Because electrochemical reductive dehalogenation is one of possible methods[17] of biaryl synthesis, the presented paper is primarily devoted to electrochemical reduction of **1**–**3** on mercury and platinum electrodes under various conditions. We also decided to prepare the 3-iodo derivative **3**, since the mentioned 3-halo-1-benzothiophene derivatives **1**–**3** represent potential precursors to a new group of axially chiral compounds.

Eletrochemical reduction of thiophene and 1-benzothiophene derivatives has been the subject of a marginal interest[18–20]. On the other hand, electrochemical studies of mono-, di-, tri- and tetrahalothiophene derivatives[21–23] using various electrode materials showed that the halogen atom is reduced before the thiophene ring and the ease of the carbon–halogen bond reduction decreases in the order C–I > C–Br > C–Cl, which is in agreement with the corresponding bond dissociation energies and with the order of halogen reduction in other haloaromatic derivatives.

RESULTS AND DISCUSSION

Synthesis

The starting methyl 3-chloro- (**1**) and 3-bromo-1-benzothiophene-2-carboxylates (**2**) were prepared by the procedures described earlier[12–16]. The new 3-iodoester **3** was obtained by the Meyers oxazoline method[24–28] starting with the chloride **6**[29] (Scheme 2). Acylation of 2-amino-2-methylpropan-1-ol afforded the corresponding amide **7** in 50% yield. Its cyclization to oxazoline **8** was achieved by treatment with thionyl chloride in a high yield of 90%. Regioselective oxazoline-mediated lithiation of **8** with *tert*-butyllithium gave rise to the lithium salt, which was subsequently trapped with iodine to form the 3-iodooxazoline **9** (yield 73%). Hydrolysis of the oxazoline system gave rise to the 3-iodoacid **10** (yield 80%) which was esterified with diazomethane to afford the required ester **3** in 68% yield.

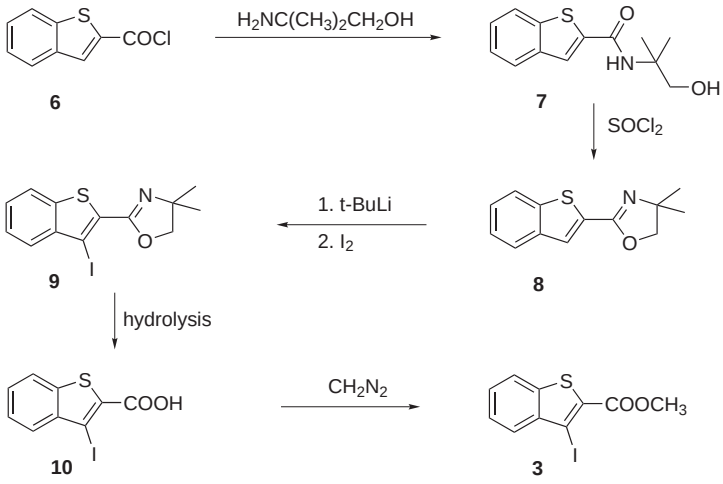

SCHEME 2

The expected products of electrochemical reduction, *i.e.* diester **4** and the reduced product **5**, were prepared by independent methods[11,30].

Electrochemical Investigation at Mercury Electrodes

In order to be able to identify the expected products eventually in the course of the reduction of halobenzothiophenes **1**–**3**, compounds **4** and **5** were studied first.

The polarographic curve of the methyl 1-benzothiophene-2-carboxylate (HBT; **5**) exhibits three reduction waves. The first at –1.90 V (SCE) is a diffusion-controlled, one-electron reversible wave. The other two more negative waves (at –2.43 and –2.73 V, not well developed) were not studied in detail. On the cyclic voltammogram, a corresponding reversible couple of peaks (Fig. 1, curve *a*) were observed suggesting the process (*1*).

$$HBT + e \rightleftharpoons HBT^{\bullet -} \qquad (1)$$

The polarographic curve of dimethyl 3,3′-bi(1-benzothiophene)-2,2′-dicarboxylate (BT_2; **4**) exhibits two reduction waves in the potential region below –2 V (SCE). The first located at –1.67 V (SCE) and the second at –1.87 V (SCE), are both diffusion-controlled one-electron waves. On the cyclic voltammogram, two corresponding reversible couples of peaks were ob-

served (Fig. 1, curve *b*). The more positive value of the first reduction potential (with respect to compound **5**) points to the existence of a larger delocalized system, which is able to consecutively accommodate two electrons. From the observed reversibility of both steps it is evident that besides electron transfers no other chemical changes occur and the formed anion-radical and dianion are stable species (Eqs (*2*), (*3*)).

$$BT_2 + e \rightleftharpoons BT_2^{\bullet -} \qquad (2)$$

$$BT_2^{\bullet -} + e \rightleftharpoons BT_2^{2-} \qquad (3)$$

The first reduction step of methyl 3-chloro-1-benzothiophene-2-carboxylate (ClBT; **1**) proceeds at the potential –1.56 V (*vs* SCE). The corresponding polarographic wave (Fig. 2, curve *a*) is a two-electron one, comparing its limiting current with those of a standard compound – 9,10-diphenylanthracene, exhibiting two one-electron reversible waves. The wave is diffusion-controlled with a linear dependence of the limiting current on concentration in the 1×10^{-5} to 1×10^{-3} M range. The linear dependence of log $[(I - I_0)/(I - I_{lim})]$ *vs E* (logarithmic analysis, where *I* is the actual current, I_0 is corresponding charging current, I_{lim} is limiting diffusion current and *E* is potential) proves, that at these potentials only one process proceeds with the same rate-determining step (RDS; Fig. 3). The cyclovoltammetric curve exhibits a corresponding cathodic peak at –1.61 V (Fig. 4,

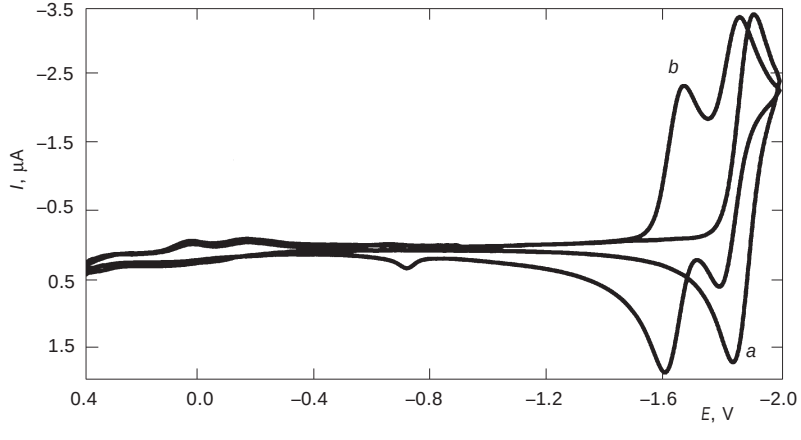

FIG. 1
Cyclic voltammetry on HMDE in 0.1 M DMF/TBAHFP, $v = 200$ mV s^{-1}, concentration 1×10^{-3} mol l^{-1}. *a* HBT, *b* BT_2

curve *a*). During the back scan, no re-oxidation anodic counterpeak was observed. However, two new anodic peaks appeared at potentials –0.10 and +0.19 V, the heights of which increase with the time of electrolysis on the first reduction wave. Addition of tetrabutylammonium chloride proved that these anodic peaks correspond to the growing content of chlorides (forming insoluble compounds with mercury).

The second wave on the polarogram represents a one-electron process at the potential –1.90 V, *i.e.* at the same potential as that of one of the possi-

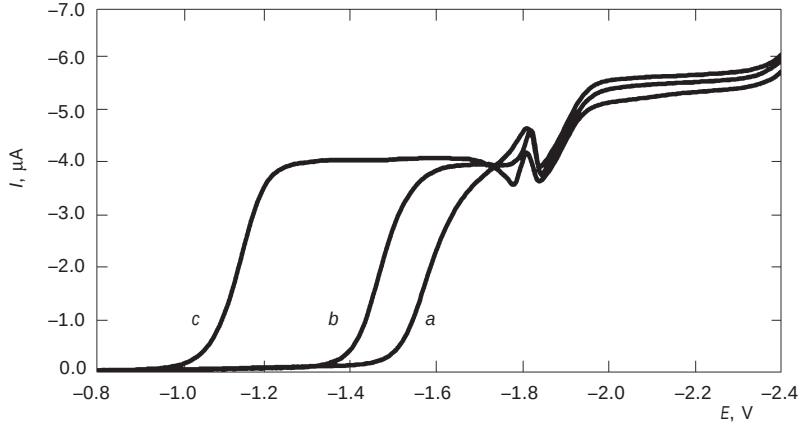

FIG. 2

DC polarography on DME in 0.1 M DMF/TBAHFP, v = 5 mV s^{-1}, concentration 1 × 10^{-3} mol l^{-1}. *a* ClBT, *b* BrBT, *c* IBT

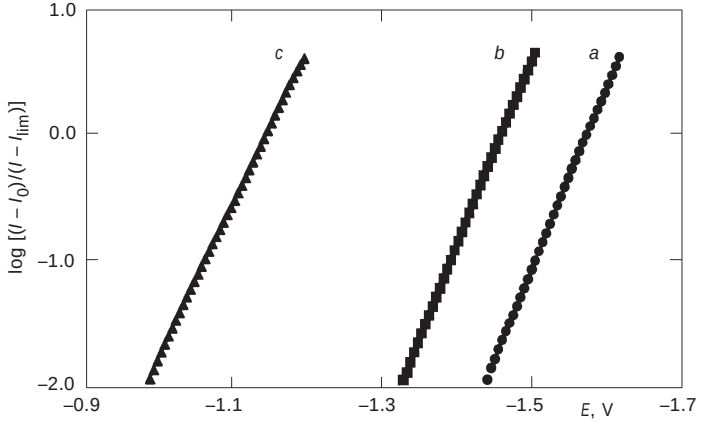

FIG. 3

Logarithmic analysis of DC polarographic waves of *a* ClBT, *b* BrBT, *c* IBT

ble products, HBT (**5**). Similarly, the cyclic voltammogram at these potentials exhibits a reversible couple of peaks identical with that of HBT.

DC polarography of methyl 3-bromo-1-benzothiophene-2-carboxylate (BrBT; **2**) exhibits its first reduction wave at –1.47 V (*vs* SCE), hence at a value by 90 mV less negative than ClBT (Fig. 2, curve *b*). This shift is the only substantial difference from the behavior of ClBT. The wave corresponds to a two-electron irreversible diffusion-controlled process. Analogously to ClBT, the linear dependence of log $[(I - I_0)/(I - I_{lim})]$ *vs* E proves that only one process proceeds with the same RDS (Fig. 3). The cyclovoltammetric curve exhibits the first cathodic peak at –1.52 V. During the back scan, no re-oxidation anodic counterpeak was observed, but two new anodic peaks appeared at potentials –0.12 and +0.22 V (Fig. 4, curve *b*). This corresponds to the presence of bromide anions (checked analogously to the ClBT by addition of tetrabutylammonium bromide).

The second wave on the polarogram represents a one-electron process at the potential –1.90 V, *i.e.* at the same potential as HBT. The cyclic voltammogram exhibits likewise a reversible couple of peaks identical with that of HBT at these potentials.

The electrochemical behavior of methyl 3-iodo-1-benzothiophene-2-carboxylate (IBT; **3**) was very close to that of ClBT and BrBT. DC polarography of IBT exhibits the first reduction wave at –1.14 V (*vs* SCE), hence at a value by 420 mV less negative than ClBT (Fig. 2, curve *c*). The wave corresponds again to a two-electron irreversible diffusion-controlled process. The linear dependence of log $[(I - I_0)/(I - I_{lim})]$ also proves that only

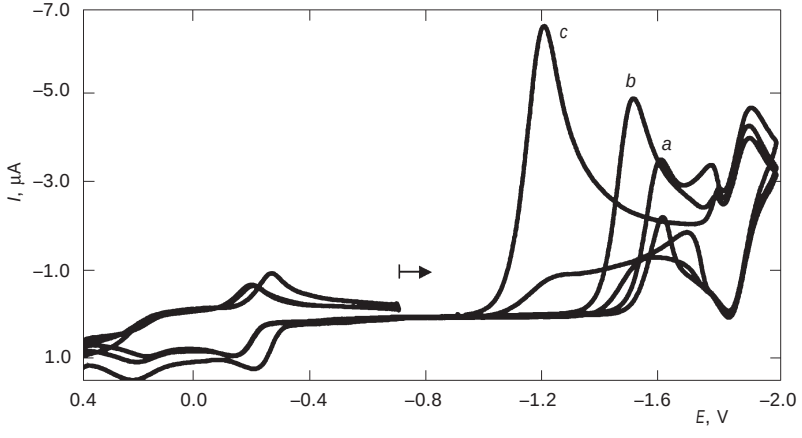

FIG. 4

Cyclic voltammetry on HMDE in 0.1 M DMF/TBAHFP, v = 200 mV s^{-1}, concentration 1×10^{-3} mol l^{-1}. *a* ClBT, *b* BrBT, *c* IBT

one process proceeds with the same RDS (Fig. 3). The cyclovoltammetric curve exhibits the first cathodic peak at the potential E_p = –1.21 V. During the back scan, no re-oxidation anodic counterpeak was observed; new anodic peaks appeared at potentials –0.17 and +0.24 V, corresponding to the presence of iodide anions.

The second wave on the polarogram represents a one-electron process at potential –1.90 V, *i.e.* at the potential of HBT. Similarly, the cyclic voltammogram exhibits at these potentials a reversible couple of peaks identical with that of HBT (Fig. 4, curve *c*).

Other features: At the potentials between –1.7 and –1.9 V, *i.e.* after the first reduction wave and close before the second wave corresponding to the common product HBT, a similar break on the limiting current is observed with all derivatives **1**–**3** (*cf.* Fig. 2). The same effect appears also on the cyclic voltammogram (*cf.* Fig. 4): at lower scan rates (50 mV s^{-1}), the curves cross, but this totally disappears at scan rates higher than 1 V s^{-1} . This behavior can be attributed to a relatively slow adsorption/desorption process of halogenated species at the electrode surface.

Addition of proton donors (water, acetic acid) has only a small effect on the electrochemical behavior of **1**–**3**. For all the studied compounds, the first two-electron wave is slightly shifted towards less negative potentials with increasing concentration of the proton donor (without a change in the limiting current) and the adsorption break at potentials from –1.7 to –1.9 V gradually disappears, most probably due to changes in solvation of molecules and in the double layer structure. At more negative potentials, the current of the proton reduction is observed.

Electrochemical Investigation at Platinum Electrodes

The reduction of methyl 1-benzothiophene-2-carboxylate (**5**) on rotating platinum disk electrode (RDE) proceeds in one diffusion-controlled, one-electron reversible wave at half-wave potential $E_{1/2}$ = –1.90 V (SCE). The cyclic voltammogram exhibits a reversible couple of peaks at potential E_p = –1.92 V.

The reduction of dimethyl 3,3′-bi(1-benzothiophene)-2,2′-dicarboxylate (BT_2; **4**) on RDE proceeds in two diffusion-controlled, one-electron reversible waves at $E_{1/2}$ (1) = –1.67 V (SCE) and $E_{1/2}$ (2) = –1.89 V. The cyclic voltammogram exhibits two reversible couples of peaks at E_p (1) = –1.68 V and E_p (2) = –1.88 V (SCE). The identical electrochemical behavior of the two standards **4** and **5** at platinum and mercury electrodes shows that the

mechanism follows the same pattern without any interaction with the electrode material.

Methyl 3-chloro-1-benzothiophene-2-carboxylate (**1**) is reduced at the RDE in two waves (Fig. 5, curve *a*). The first wave at –1.6 V corresponds to the reduction of the parent compound, the second one (at –1.90 V) to the reduction of HBT (checked by addition of authentic HBT). The limiting current, however, depends on the scan rate: at lower scan rates the waves decrease. This effect points to the fact that the electrode surface is blocked by a film of formed products. This passivation is also more pronounced at higher concentrations of the substrate. For reactivation of the electrode, a positive polarization is needed. The electrode passivation is also evident from the ratio of limiting currents of the first and of the second wave (Fig. 5, curve a): instead of the 2:1, the ratio 1:1 is observed, the first wave being much lower than expected for a two-electron process.

The cyclovoltammetric curve of ClBT (Fig. 6, curve *a*) exhibits the first cathodic peak at –1.67 V without any anodic counterpeak. The second reduction process is reversible at E_p = –1.92 V and corresponds again to the one-electron reduction of HBT.

In the case of methyl 3-bromo-1-benzothiophene-2-carboxylate (**2**) and methyl 3-iodo-1-benzothiophene-2-carboxylate (**3**), the electrode passivation is much more pronounced: the voltammetic curve of the bromo derivative **2** on RDE at a slow scan rate (5 mV s^{-1}) exhibits a current increase around –1.5 V; however, before reaching the limiting value the current declines to zero and no other wave appears. On the repeated scan without

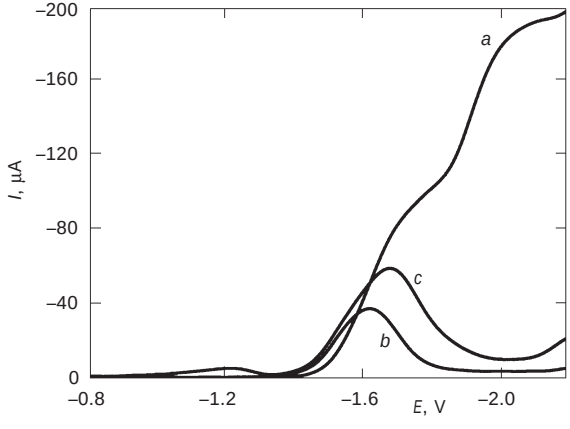

FIG. 5

Voltammetry on platinum RDE (first scans) in 0.1 M DMF/TBAHFP, v = 5 mV s^{-1}, concentration 1×10^{-3} mol l^{-1}. *a* ClBT, *b* BrBT, *c* IBT

electrode cleaning, no current is observed. An analogous effect was observed in the case of IBT (**3**): a small current appears on the first scan at –1.1 and –1.5 V, but after that the electrode is completely blocked (Fig. 5, curves *b*, *c*).

The cyclic voltammogram of BrBT (which is recorded at 200 mV s^{-1}) is completely analogous to that of ClBT, *i.e.*, two reduction processes are observed at this scan rate. The first one is irreversible at –1.67 V and the second one is reversible at –1.92 V. The IBT shows the same result (Fig. 6). The only difference is that on the first scan an additional, not well reproducible adsorption-controlled current (linearly dependent on scan rate) is observed between –0.9 and –1.3 V, which disappears in the second and following scans and which can be restored when switching a more positive potential than +0.4 V.

From the investigation of 3-haloesters **1**–**3** on platinum electrodes arises that the reduction is complicated by a slow electrode-assisted reduction in the adsorbed state leading to formation of an insoluble insulating (polymer) film on the electrode preventing further reduction. This reaction is most probably related to adsorption of the starting compounds on platinum covered with surface oxides.

The electrochemical investigation on mercury as well as on platinum electrodes under the above-discussed conditions shows that reduction of haloesters **1**–**3** is a two-electron ECE (electron transfer – chemical follow-up reaction – electron transfer) process. After the uptake of the first electron,

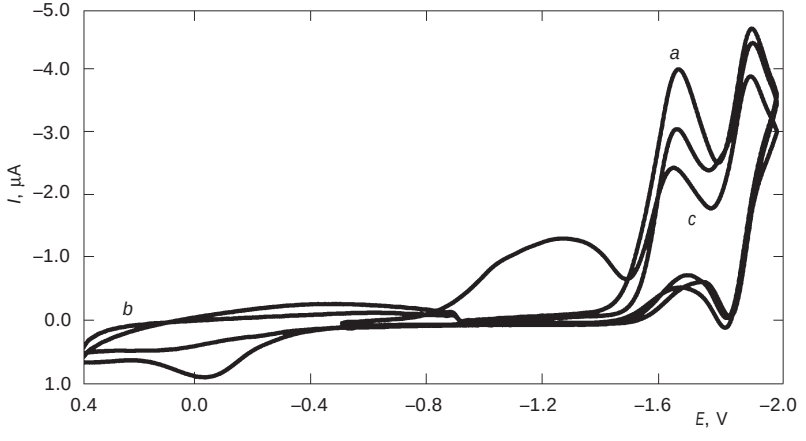

FIG. 6

Cyclic voltammetry on platinum stationary electrode in 0.1 M DMF/TBAHFP, v = 200 mV s^{-1}, concentration 1×10^{-3} mol l^{-1}. *a* ClBT, *b* BrBT, *c* IBT

the formed radical-anion splits off the halide anion (good leaving group) and forms a neutral radical. This is immediately reduced by the second electron and subsequently protonated under the formation of a dehalogenated (reduced) product, HBT (**5**) – see Eqs (*4*)–(*7*). The latter is the only product detected in all performed electroreduction reactions. Formation of the BT_2 dimer was never observed under these conditions. The data are summarized in Table I.

$$\underset{(X = Cl, Br, I)}{XBT + e} \rightleftharpoons XBT^{\bullet -} \quad E_1 \tag{4}$$

$$XBT^{\bullet -} \longrightarrow BT^{\bullet} + X^{-} \tag{5}$$

$$BT^{\bullet} + e \rightleftharpoons BT^{-} \quad E_2 \quad (|E_2| < |E_1|) \tag{6}$$

$$BT^{-} + H^{+} \longrightarrow HBT \tag{7}$$

After the first wave, the reversible one-electron reduction of HBT (*1*) follows always at the same potential (E_{pc} = –1.92 V *vs* SCE).

The splitting of the radical-anion is most probably the RDS. The cyclic voltammograms at HMDE show, that E_p of the first peak is shifted to more negative potentials with increasing scan rate. Analysis of the E_p on log *v*

TABLE I
Electrochemical reduction data (in V) of compounds **1**–**3** on mercury and platinum electrodes (DMF/TBAHFP *vs* SCE)

Compound	Mercury				Platinum	
	polarography		cyclic voltammetry		cyclic voltammetry	
	$E_{1/2}(1)$	$E_{1/2}(2)$	$E_p(1)$	$E_p(2)$	$E_p(1)$	$E_p(2)$
CIBT	–1.56	–1.89	–1.61	–1.92	–1.67	–1.92
BrBT	–1.47	–1.90	–1.52	–1.92	–1.67	–1.92
IBT	–1.14	–1.90	–1.21	–1.92	–1.66	–1.92
HBT	–	–1.90	–	–1.92	–	–1.92
BT_2	–1.66	–1.86	–1.68	–1.88	–1.68	–1.87

(scan rate) dependence shows linearity (for scan rates 50 mV s^{-1} to 50 V s^{-1}) with the slope 15 mV per decade for ClBT, 35 mV/dec for BrBT and 45 mV/dec for IBT (Fig. 7). This behavior is consistent with the ECE mechanism[31] since even at the scan rate 1 kV s^{-1}, no anodic counterpeak is observed. Thus, the rate constants of the anion radical splitting are expected[32] to be higher than 10^5 s^{-1}.

From a comparison of results with mercury and platinum electrodes, two differences appear:

1. In contrast to the reduction on mercury, the reduction of haloesters **1**–**3** at platinum electrodes proceeds at more negative potentials and, moreover, at the same potential –1.67 V (*cf.* Table I). The interpretation is based on the fact that at both electrode materials the reduction is "electrode assisted", *i.e.*, a specific interaction between the substrate and the electrode proceeds prior to the electron transfer. The adsorption of haloesters on mercury electrode proceeds *via* the halogen atom under the formation of an activated σ-complex; therefore, the influence of the halogen on the reduction potential is substantial. On the other hand, the surface of platinum electrode is known through its affinity to π-systems; therefore, the adsorption *via* the aromatic ring is expected. In the latter case, the difference in substituents (Cl, Br, I) does not play a role and all the studied substances behave similarly.

2. Simultaneously with the diffusion-controlled reductive dehalogenation on platinum (Eqs (*4*)–(*7*)), another reduction proceeds yielding most probably polymeric species blocking the electrode. The latter reaction involves

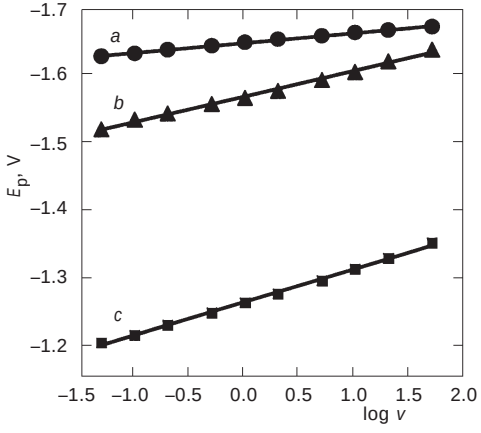

FIG. 7

Dependence of E_p (CV in 0.1 M DMF/TBAHFP on mercury electrode) on log *v*. *a* ClBT, *b* BrBT, *c* IBT

only adsorbed molecules and is much slower than the diffusion-controlled main process, because it manifests itself only at low scan rates.

On the other hand, on mercury at potentials –1.7 to –1.9 V, a break (an anodic jump) of the limiting current and a crossing of cyclic voltammograms occur. This is closely associated with the presence of the halogenated species, since during reduction of neat HBT (**5**) such breaks and crossings are not observed. This effect (*cf.* Figs 2 and 3) is most probably caused by adsorption/desorption phenomena of halogenated reduction intermediates in their activated state (marked by asterisk).

$$\mathrm{XBT} \rightleftharpoons (\mathrm{XBT})_{ads} \qquad (8)$$

$$(\mathrm{XBT})_{ads} + 2\ \mathrm{e} + \mathrm{H^+} \longrightarrow (\mathrm{HXBT^*})^-_{ads} \quad \text{(the first wave)} \qquad (9)$$

$$(\mathrm{HXBT^*})^-_{ads} + \mathrm{e} \longrightarrow (\mathrm{HBT})^-_{ads} + \mathrm{X^-} \quad \text{(start of the second wave)} \qquad (10)$$

$$(\mathrm{HBT})^-_{ads} \longrightarrow \mathrm{HBT} + \mathrm{e} \quad \text{(anodic jump)} \qquad (11)$$

$$\mathrm{HBT} + \mathrm{e} \rightleftharpoons \mathrm{HBT^{\bullet -}} \quad \text{(regular second wave)} \qquad (1)$$

In any case, no blocking adsorbed film is formed on mercury electrodes.

Sonovoltammetry at Platinum Electrodes

Sonication, due to its microjets directed to electrode surface[33,35,36], is the most efficient tool for removal of layers of products deposited at the electrode, *i.e.* for cleaning and reactivation of the electrode surface. This use is demonstrated on the reduction of IBT at platinum electrodes (Fig. 8). The slow cyclic voltammogram exhibits three waves on the first scan (as mentioned above): an irreversible wave at –1.67 V followed by the reversible couple of HBT at –1.92 V and a not well developed process between –0.9 and –1.4 V (curve *a*). On the second scan (without cleaning), the current between –0.9 and –1.4 V disappears (curve *b*). When stirring is applied (bubbling argon), only the diffusion-controlled current of waves at –1.67 and –1.92 V increases (with oscillations due to the bubbling), whereas the current around –1.4 V remains on the same level and without oscillations. This points to the fact that the reaction leading to fouling of the electrode is slow, hence the reduction is kinetically controlled (curve *c*). When

sonication is applied (curve *d*), a strong increase in the current is observed (starting at the potential –1.2 V), which manifests the continuous reactivation of the electrode.

Constant Potential Electrolysis

Electrolysis in small scale at DME (dropping mercury electrode), HMDE (hanging mercury drop electrode), RDE (rotating disk electrode) and stationary Pt electrode yielded HBT as the sole reduction product. However, theoretically a concurrent one-electron mechanism Edim[37] (electron transfer – dimeration) should also be considered, where the neutral radicals generated in Eq. (*5*) dimerize instead of a consecutive reduction.

$$2\ BT^{\bullet} \longrightarrow BT_2 \qquad (12)$$

The key step for accomplishing such a reaction is to prevent the second electron transfer and to favour the coupling reaction. This may be achieved in preparative electrolysis, *e.g.*, by increased concentration and/or by fast removal of the primary radical-anion from the electrode surface before its splitting and thus by shifting the reaction from the heterogeneous conditions to homogeneous ones.

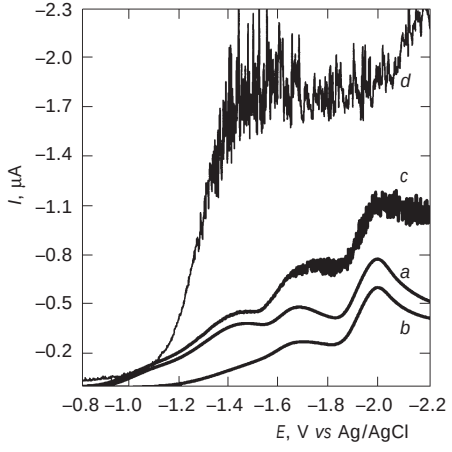

FIG. 8

Sonovoltammetry of 3×10^{-3} M IBT in 0.1 M DMF/TBAHFP on platinum electrode, v = 5 mV s^{-1}. First scan without stirring (*a*), second scan without stirring (*b*), first scan with stirring by bubbling argon (*c*), first and all repeated scans under sonication (*d*)

Electrolyses at a Mercury Pool Electrode

Haloesters **1**–**3** were reduced on a stirred mercury pool electrode at potentials of the limiting current of their first reduction wave up to 95% conversion. The changes in concentrations were followed during the electrolysis by polarography and by HPLC. Simultaneously, the number of passed electrons was calculated (results are summarized in Table II). HPLC analysis of products revealed the formation of HBT as the only product and no BT_2 dimer was detected.

The same series of electrolyses was performed in the presence of a redox mediator in order to change the direct heterogeneous reduction on the electrode to a homogeneous indirect process in the bulk and thus to promote the eventual dimerization. The mediator forms at the electrode a stabile radical-anion, which can then reduce the substrate homogeneously.

$$M + e \rightleftharpoons M^{\bullet -} \qquad (13)$$

$$M^{\bullet -} + XBT \rightleftharpoons M^{\bullet} + XBT^{-} \qquad (14)$$

etc.

Two suitable mediators were found: fluoren-9-one and 4-cyanobenzophenone. Both the mediators are reduced at slightly more positive potentials than BrBT in one reversible one-electron step. After addition of the substrate, the reduction current of the mediator increases and the reversibility is partly lost, whereas the original wave of BrBT disappears (Fig. 9). In comparison with the heterogeneous electrolysis on mercury pool, the mediated process proceeds much faster, at more positive potentials and with 100% conversion. The only product found after the mediated preparative electrolysis was the dehalogenated product HBT with two consumed electrons per molecule of the substrate (Table II).

Electrolyses at Platinum Electrode with Sonication

The ultrasound sonication is a convenient method for removing the blocking film of products deposited on the platinum electrode during electroreduction of compounds **1**–**3** and thus for performing a preparative electrolysis. Besides the effect of reactivation of the electrode, the microjets cause also a very fast transport of substrate to the electrode and of intermediates and products away from the electrode. This generally offers a possibility of the change of mechanism from the ECE to EDim, since the primary radical-

anion is transferred to the bulk of solution and its consecutive reduction at the electrode is partly prevented.

The compounds **1**–**3** were electrolyzed under sonication at small platinum gauze electrode, at large platinum foil electrode and, for comparison, also at mercury pool electrode. The electrolyses at platinum electrodes proceeded successfully, the polarographic as well as the HPLC analysis of products and the coulometric measurement revealed that the only product under these conditions was HBT under the consumption of approximately two electrons per molecule.

TABLE II
Results of controlled potential preparative electrolyses on mercury pool electrode

Compound	Mediator	Potential V *vs* SCE	Concentration mol l^{-1}	Time min	Conversion %	Charge passed C	*n*
CIBT	–	–1.70	8.82×10^{-3}	50	94	14.5	1.82
BrBT	–	–1.60	7.38×10^{-3}	45	92	11.6	1.77
BrBT	Fluoren-9-one	–1.30	7.38×10^{-3}	20	100	14.3	2.01
BrBT	*p*-CNBP[a]	–1.38	7.38×10^{-3}	22	100	14.2	2.00
IBT	–	–1.40	6.29×10^{-3}	60	95	10.3	1.79

[a] 4-Cyanobenzophenone.

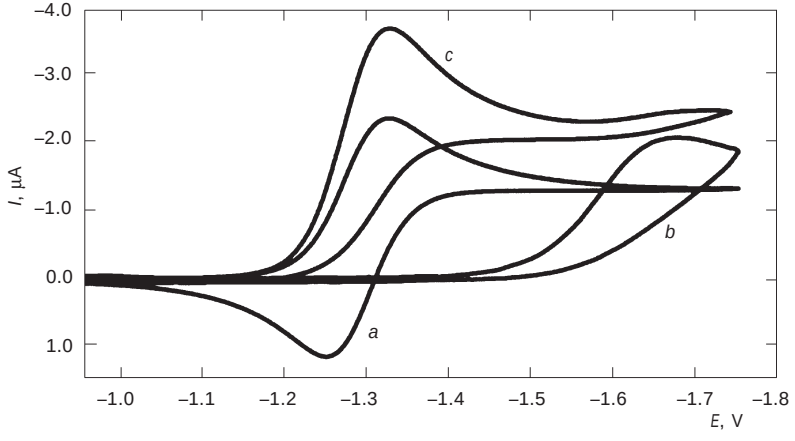

FIG. 9
Cyclic voltammetry in 0.1 M DMF/TBAHFP, v = 10 mV s^{-1}, concentration 3×10^{-3} mol l^{-1}. *a* fluorenone, *b* BrBT, *c* fluorenone + BrBT

Conclusions

A new compound, iodo ester **3** has been synthesized using the procedure of regioselective oxazoline-mediated lithiation of 1-benzothiophene derivative **8**.

The electroreduction of haloesters **1**–**3** and their possible products **4**, **5** were investigated at mercury and platinum electrodes using polarography, cyclic voltammetry and RDE methods in anhydrous dimethylformamide. The reduction in divided cells follows the ECE mechanism, where the primary radical anion is split into halide anion and neutral heterocyclic radical, which is immediately reduced by the second electron and protonated. The EDim mechanism leading to the dimeric species **4** was not observed under the above conditions. The only reduction product is HBT (**5**).

Reduction at both materials are electrode assisted. Whereas at mercury electrodes a halogenated intermediate is adsorbed, at platinum a polymeric film blocking the electrode is formed. The differences in reduction potentials were interpreted in terms of electrode–substrate interaction.

The electropreparative use of these reductions was proved by controlled potential electrolyses under various conditions. At mercury electrodes the indirect, mediated reduction proceeds at more positive potentials and much faster than the direct heterogeneous process. The major drawback of platinum electrode is its fouling by formation of an insulating film of products. These effects are usually overcome by pulsing the potential to extreme positive/negative values. This treatment, however, leads to additional irreproducible electrode reactions. In this contribution we successfully used the sonication for removal of products from the surface of the electrode and thus enabling electrolysis.

EXPERIMENTAL

Instrumentation and Methods

For electrochemical investigation of compounds **1**–**5** at mercury electrodes, DC polarography with dropping mercury electrode (DME), cyclic voltammetry with hanging mercury drop electrode (HMDE) and controlled potential electrolysis (CPE) with mercury pool electrode were used. For investigation at platinum electrodes voltammetry on the Pt-rotating disk electrode (RDE), cyclic voltammetry on stationary platinum electrode and controlled potential electrolysis with platinum foil and platinum net electrode were used. For comparison, experiments with sonication were also performed. All measurements proceeded in divided three-compartment cells with saturated calomel electrode (SCE) as a reference and platinum foil as an auxiliary electrode using the potentiostat PGSTAT 30 (EcoChemie, Netherland). The solution was deaerated by purging with pure argon. For sonoelectrochemical investigation a special cell[35] was utilized. As a source of sonication, an ultrasound generator SON 200 (20 kHz,

maximum 200 W) was used together with a piezoelectric titanium horn, 14 mm in diameter (EL-MEDICA, Kladno, Czech Republic).

Melting points were determined on a Leica VM TG block and are uncorrected. Elemental analyses were carried out on a Perkin–Elmer 2400. IR spectra were recorded on a Nicolet 740 FT-IR spectrometer in chloroform or KBr. NMR spectra were recorded on a Varian Gemini 300 HC (300 MHz). Deuteriochloroform or DMSO-d_6 were used as solvents; solvent signals served as internal standards. Chemical shifts δ are given in ppm, spin–spin interaction constants J in Hz. TLC analyses were performed on glass plates with a layer of silica gel Kieselgel GF_{254} (Merck).

All electrochemical measurements were realized in 0.1 M solution of tetrabutylammonium hexafluorophosphate (TBA HFP) in anhydrous dimethylformamide (DMF). DMF was freshly distilled from CaH_2 and stored over molecular sieves. Tetrahydrofuran and diethyl ether for synthesis were distilled from sodium and benzophenone. Ester **1** (m.p. 79–80 °C; ref.[38] gives 81.3 °C) was obtained analogously to refs[12,13]. The bromo ester **2** (m.p. 69–70.5 °C; ref.[16] gives 71.5 °C) was prepared by a three-step route described in refs[14–16]. Dimethyl 3,3′-bi(1-benzothiophene)-2,2′-dicarboxylate (**4**) was obtained according to ref.[11] in 58% yield, m.p. 208–210 °C. Methyl 1-benzothiophene-2-carboxylate (**5**) was prepared according to ref.[30] in 37% yield, m.p. 71–72 °C. Other chemicals were commercial and used as received.

N-(2-Hydroxy-1,1-dimethylethyl)-1-benzothiophene-2-carboxamide (**7**)

To a solution of 1-benzothiophene-2-carbonyl chloride[29] (**6**; 11.0 g, 56 mmol) in dry dichloromethane (150 ml), 2-amino-2-methylpropan-1-ol (10.0 g, 112 mmol) was added dropwise under stirring at 0 °C. The mixture was then stirred at room temperature for 12 h, and washed successively with cold water (200 ml), 5% aqueous hydrochloric acid (50 ml) and saturated aqueous sodium chloride solution (50 ml). The organic layer was dried with anhydrous magnesium sulfate and evaporated to dryness. Crystallization from toluene afforded 7.0 g (50%) of amide **7**, m.p. 129.5–132 °C. For $C_{13}H_{15}NO_2S$ (249.3) calculated: 62.62% C, 6.06% H, 5.62% N; found: 62.46% C, 5.98% H, 5.44% N. IR: 3413 (OH), 2969, 2933, 1645 (CO), 1506, 1 458, 1295. ^{1}H NMR: 1.44 s, 6 H (CH_3); 3.72 d, 2 H, J = 6.5 (CH_2); 4.16 t, 1 H (OH); 6.19 s, 1 H (NH); 7.39 dt, 1 H; 7.43 dt, 1 H; 7.73 s, 1 H (H-3); 7.82 dd, 1 H, J_1 = 8.8, J_2 = 2.2; 7.86 dd, 1 H.

2-(1-Benzothiophen-2-yl)-4,4-dimethyl-4,5-dihydrooxazole (**8**)

Amide **7** (6.0 g, 24.1 mmol) in toluene (60 ml) was treated with thionyl chloride (3.0 g, 25.3 mmol) under stirring at 0 °C. Stirring was continued at 0 °C for 0.5 h and at room temperature for 12 h. The mixture was diluted with toluene (60 ml) and 10% aqueous sodium hydroxide (30 ml) was added. After 20 min stirring the organic layer was separated, washed subsequently with water (50 ml), saturated aqueous sodium chloride solution (50 ml) and dried with anhydrous magnesium sulfate. After evaporation of toluene, the residue was triturated with hexane (15 ml), the precipitate was filtered off and washed with cold hexane. Oxazole **8** (5.0 g; 90%) was obtained, m.p. 55–56 °C. For $C_{13}H_{13}NOS$ (231.3) calculated: 67.50% C, 5.66% H, 6.06% N; found: 67.41% C, 5.38% H, 5.89% N. IR: 3057, 2971, 1356, 1210, 1028. ^{1}H NMR: 1.41 s, 6 H (CH_3); 4.15 s, 2 H (CH_2); 7.37 dt, 1 H; 7.40 dt, 1 H; 7.81 s, 1 H (H-3); 7.82 m, 1 H; 7.86 dd, 1 H, J_1 = 8.8, J_2 = 2.2.

2-(3-Iodo-1-benzothiophen-2-yl)-4,4-dimethyl-4,5-dihydrooxazole (**9**)

To a solution of oxazole **8** (4.0 g, 17.3 mmol) in dry THF (60 ml), *tert*-butyllithium (17.3 ml of 1.5 M solution in pentane; 25.9 mmol) was added dropwise under stirring at –78 °C in nitrogen atmosphere. The mixture was stirred for 1 h and the formed lithium salt was trapped with a solution of iodine (6.56 g, 25.9 mmol) in THF (20 ml). The mixture was stirred at room temperature for 1 h, the reaction was quenched by addition of 5% aqueous sodium thiosulfate (100 ml) and the product was extracted with chloroform (3 × 50 ml). The organic solution was dried with anhydrous magnesium sulfate, evaporated to dryness and the residue was purified by column chromatography (silica gel, toluene) to afford 4.52 g (73%) of compound **9**, m.p. 48–49 °C (hexane). For $C_{13}H_{12}INOS$ (357.2) calculated: 43.71% C, 3.39% H, 3.92% N; found: 43.45% C, 3.21% H, 3,88% N. IR: 3020, 2978, 1516, 1355, 1028. ^{1}H NMR: 1.43 s, 6 H (CH_3); 4.20 s, 2 H (CH_2); 7.45 dt, 1 H; 7.47 dt, 1 H; 7.79 dd, 1 H, J_1 = 8.8, J_2 = 2.2; 7.89 dd, 1 H.

3-Iodo-1-benzothiophene-2-carboxylic Acid (**10**)

A mixture of oxazole **9** (3.0 g, 8.4 mmol) and 10% aqueous hydrochloric acid (60 ml) was heated to reflux for 15 min and then cooled to room temperature. The formed precipitate was filtered off, washed with cold water (10 ml) and added to a solution of 20% sodium hydroxide in 50% aqueous methanol (60 ml). After heating to reflux for 30 min, the solution was cooled to room temperature and acidified with 10% aqueous hydrochloric acid. The precipitate was filtered off, washed with water and dried *in vacuo*. Acid **10** (2.05 g; 80%) was obtained, m.p. 237–240 °C. For $C_9H_5IO_2S$ (304.1) calculated: 35.55% C, 1.66% H; found: 35.37% C, 1.71% H. IR (KBr): 3013, 1695 (CO), 1301, 1260. ^{1}H NMR (DMSO): 7.86 m, 1 H; 7.90 m, 1 H; 8.03 dd, 1 H, J_1 = 8.8, J_2 = 2.2; 8.06 dd, 1 H.

Methyl 3-Iodo-1-benzothiophene-2-carboxylate (**3**)

To a mixture of acid **10** (2.25 g, 7.40 mmol) in dry ether (30 ml), an etheral solution of freshly prepared diazomethane was added dropwise under stirring untill the yellow color persisted for 20 min. The solution was evaporated to dryness and crystallization from methanol afforded 1.60 g (68%) of ester **3**, m.p. 92–93.5 °C. For $C_{10}H_7IO_2S$ (318.1) calculated: 37.75% C, 2.22% H, 38.89% I; found: 37.64% C, 2.16% H, 37.55% I. IR: 3028, 1725 (CO), 1503, 1238, 1224, 1058. ^{1}H NMR: 3.98 s, 3 H (OCH_3); 7.52 m, 2 H (H-5, H-6); 7.82 dd, 1 H, J_1 = 8.8, J_2 = 2.2 (H-7); 7.96 dd, 1 H, J_1 = 8.8, J_2 = 2.2 (H-4).

Financial support from the Grant Agency of the Czech Republic (project No. 202/02/0840), the Grant Agency of the Academy of Sciences of the Czech Republic (grant No. A4040304) and the Ministry of Education, Youth and Sports (project No. MSM 223100001) is gratefully acknowledged.

REFERENCES

1. Miyaura N., Suzuki A.: *Chem. Rev.* **1995**, *95*, 2457.
2. Negishi E.: *Acc. Chem. Res.* **1982**, *15*, 340.
3. Farina V.: *Pure Appl. Chem.* **1996**, *68*, 73.
4. Fanta P. E.: *Synthesis* **1974**, 9.

5. Houben–Weyl: *Methods of Organic Chemistry*, Vol. E21a, *Stereoselective Synthesis* (G. Helmchen, R. W. Hoffmann, J. Mulzer and E. Schaumann, Eds). G. Thieme Verlag, Stuttgart 1995.
6. Noyori R., Takaya H.: *Acc. Chem. Res.* **1990**, *23*, 345.
7. Bennincori T., Brenna E., Sannicolo F., Trimarco L., Antognazza P., Cesarotti E., Demartin F., Pilati T.: *J. Org. Chem.* **1996**, *61*, 6244.
8. Solladie G., Zimmermann R.: *J. Org. Chem.* **1985**, *50*, 4062.
9. Solladie G., Hugelé P., Bartsch R., Skoulios A.: *Angew. Chem., Int. Ed. Engl.* **1996**, *35*, 1533.
10. Solladie G., Hugele P., Bartsch R.: *J. Org. Chem.* **1998**, *63*, 3895.
11. Mézlová M., Petříčková H., Maloň P., Svoboda J.: *Collect. Czech. Chem. Commun.* **2003**, *68*, 1020.
12. Nič M., Havelková M., Terinek M., Paleček J., Svoboda J., Jandera A., Panajotová V., Kuchař M.: *Cesk. Farm.* **1999**, *48*, 281.
13. Higa T., Krubsack A. J.: *J. Org. Chem.* **1976**, *41*, 3399.
14. Smirnov-Zamkov I., Zborovskii Y. L.: *Zh. Org. Khim.* **1975**, *11*, 1776.
15. Ried W., Bender H.: *Chem. Ber.* **1955**, *88*, 34.
16. Reinecke M. G., Newsom J. G., Almqvist K. A.: *Synthesis* **1980**, 327.
17. Nedelec J.-Y., Perichon J.: *Trends Org. Chem.* **1992**, *3*, 173.
18. Gultyai V. P., Proskurovskaya I. V., Rubinskaya T. Ya., Lozanova A. V., Moiseenkov A. M., Semenovskii A. V.: *Izv. Akad. Nauk, Ser. Khim.* **1979**, *7*, 1576.
19. Pacut R. I., Miller E. K.: *J. Org. Chem.* **1986**, *51*, 3468.
20. Mairanovskii S. G., Kosychenko L. I., Litvinov V. P.: *Elektrokhimiya* **1979**, *15*, 118.
21. Brown L. W., Krupski E.: *J. Pharm. Sci.* **1963**, *52*, 55.
22. Mairanovskii S. G., Barashkova N. V., Volkenshtein Y. B.: *Sov. Electrochem.* **1965**, *1*, 60.
23. Feldmann M., Koberstein E.: *Chem.-Tech. (Heidelberg)* **1977**, *6*, 517.
24. Meyers A. I., Temple D. R.: *J. Am. Chem. Soc.* **1970**, *92*, 6644.
25. Meyers A. I., Mihelich E. D.: *J. Org. Chem.* **1975**, *40*, 3159.
26. Gschwend H. W., Haman A.: *J. Org. Chem.* **1975**, *40*, 2008.
27. Vecchia L. D., Vlattas I.: *J. Org. Chem.* **1977**, *42*, 2649.
28. Carpenter A. J., Chadwick J.: *J. Chem. Soc., Perkin Trans. 1* **1985**, 173.
29. Chapleo C. B., Myers P. L., Butler R. C. M., Davis J. A., Doxey J. C., Higgins S. D., Myers M., Roach A. G., Smith C. F. C., Stillings M. R., Welbourn A. P.: *J. Med. Chem.* **1984**, *27*, 570.
30. Beck J. R.: *J. Org. Chem.* **1972**, *37*, 3224.
31. Tipper C. F. H. in: *Electrode Kinetics: Principles and Methodology* (R. G. Compton, Ed.). Elsevier Science Ltd., Amsterdam 1986.
32. Nicholson R. S., Shain I.: *Anal. Chem.* **1964**, *36*, 706.
33. Klíma J., Bernard C., Degrand C.: *J. Electroanal. Chem.* **1995**, *399*, 147.
34. Kratochvílová K., Hoskovcová I., Jirkovský J., Klíma J., Ludvík J.: *Electrochim. Acta* **1995**, *40*, 2603.
35. Klíma J., Bernard C.: *J. Electroanal. Chem.* **1999**, *462*, 181.
36. Klíma J., Ludvík J.: *Collect. Czech. Chem. Commun.* **2000**, *65*, 941.
37. Feoktistov L. C. in: *Organic Electrochemistry* (M. M. Baizer, Ed.). M. Dekker, New York 1983.
38. Ried W., Oremek G., Ocakcioglu B.: *Justus Liebigs Ann. Chem.* **1980**, 1424.